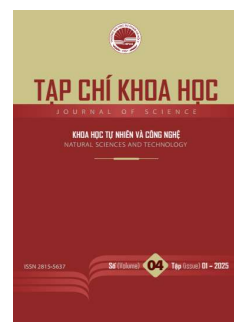




## HPU2 Journal of Sciences: Natural Sciences and Technology

Journal homepage: <https://sj.hpu2.edu.vn>



Article type: *Research article*

### The ammonium adsorption capacity of coffee husk-derived activated carbon composite with $\text{MnFe}_2\text{O}_4$

Thuy-Tien Do<sup>a\*</sup>, Thi-Huyen Nguyen<sup>a</sup>, The-Duyen Nguyen<sup>a</sup>, Huu-Tap Van<sup>b</sup>

<sup>a</sup>Hanoi Pedagogical University 2, Vinh Phuc, Vietnam

<sup>b</sup>Center for Advanced Technology Development, Thai Nguyen University, Thai Nguyen, Vietnam

#### Abstract

In this study, a composite material between  $\text{MnFe}_2\text{O}_4$  and activated carbon from coffee husks (MFO/AC) was synthesized using co-precipitate and hydrothermal methods to remove ammonium from aqueous solutions. The characteristics of MFO/AC were characterized and evaluated by scanning electron microscopy (SEM) and Fourier transform infrared spectra (FTIR). The ammonium adsorption process of MFO/AC was investigated through batch experiments, assessing parameters such as solution pH (3 ÷ 8), contact time (5 ÷ 120 min), material dosage (0.2 ÷ 3  $\text{g.L}^{-1}$ ), and initial ammonium concentration (10 ÷ 60  $\text{mg.L}^{-1}$ ). Results indicate that MFO/AC effectively adsorbs ammonium, which is attributed to the functional groups on the composite surface. The maximum ammonium adsorption capacity of MFO/AC was 15.97  $\text{mg.g}^{-1}$  at an initial ammonium concentration of 20  $\text{mg.L}^{-1}$ , pH 7, material dosage of 1.5  $\text{g.L}^{-1}$ , and contact time of 80 min. The MFO/AC composite material has the potential to be an effective agent for ammonium removal from wastewater.

**Keywords:**  $\text{MnFe}_2\text{O}_4/\text{AC}$ , ammonium, composite materials, coffee husk, activated carbon

#### 1. Introduction

Ammonium ( $\text{NH}_4^+$ ) is an essential nutrient for plants and living organisms; however, at elevated concentrations, it poses significant risks to human and animal health [1]. In recent decades, the rapid development of industry, urbanization, and population growth has led to increasing pollution of natural water sources. Agricultural activities, particularly the widespread use of fertilizers, coupled with nitrogen-rich wastewater from agricultural and domestic sources, have contributed to the contamination of groundwater with nitrogenous compounds, primarily ammonium. Although ammonium itself is not acutely toxic to humans, its transformation products (nitrite ( $\text{NO}_2^-$ ) and nitrate ( $\text{NO}_3^-$ )) are highly toxic

\* Corresponding author, E-mail: [dothuytien@hpu2.edu.vn](mailto:dothuytien@hpu2.edu.vn)

<https://doi.org/10.56764/hpu2.jos.2024.4.1.39-47>

Received date: 19-12-2024 ; Revised date: 11-3-2025 ; Accepted date: 26-3-2025

This is licensed under the CC BY-NC 4.0

[2], [3]. These compounds are formed through microbial oxidation processes during water treatment, storage, and transportation. If untreated, ammonium can be converted into nitrate in the human digestive system, potentially causing methemoglobinemia and other severe health issues, particularly in children and pregnant women. This poses a substantial risk to both aquatic ecosystems and human health [4]. Current methods for ammonium removal include adsorption, stripping towers, chemical precipitation, electrochemical treatments, and biological processes. However, stripping towers are energy-intensive, and chemical precipitation can introduce secondary pollutants. Therefore, adsorption has emerged as a preferred method for ammonium removal in recent years due to its simplicity, cost-effectiveness, and ease of operation.

MnFe<sub>2</sub>O<sub>4</sub> material with outstanding properties such as high saturation magnetization, good durability, and high catalytic activity is an effective adsorbent to remove pollutants from aqueous solutions [5]. Therefore, this material and its derivatives have been used as effective adsorbents for the removal of heavy metal ions, dyes, pesticides, and other pollutants [5]–[9]. The MnFe<sub>2</sub>O<sub>4</sub>/C nanocomposite shows excellent potential for environmental treatment due to its ability to combine the adsorption properties of both activated carbon and MnFe<sub>2</sub>O<sub>4</sub>. This combination often leads to higher adsorption efficiency and capacity than using each material alone [10]. However, the performance depends strongly on the mass ratio of activated carbon to MnFe<sub>2</sub>O<sub>4</sub> in the composite and other influencing factors. Activated carbon typically contains oxygen-based functional groups, such as carboxyl (-COOH), hydroxyl (-OH), and alcohol (-C-O), which play an important role in the adsorption process [11]. In recent years, the application of composite materials based on MnFe<sub>2</sub>O<sub>4</sub> and agricultural by-products for ammonium removal from aqueous solution has been relatively underexplored in scientific research. This study synthesized composite materials between MnFe<sub>2</sub>O<sub>4</sub> and activated carbon from coffee husks (MnFe<sub>2</sub>O<sub>4</sub>/AC) by the co-precipitate and hydrothermal method to remove ammonium in aqueous solution. The ammonium adsorption capacity of MnFe<sub>2</sub>O<sub>4</sub>/AC was evaluated by examining factors such as pH, adsorption time, adsorbent content, and initial ammonium concentration, allowing for an estimation of the composite material's maximum ammonium adsorption capacity.

## 2. Experimental

### 2.1. Chemicals and experimental equipment

The main raw materials used in this study are MnCl<sub>2</sub>·4H<sub>2</sub>O and FeCl<sub>3</sub>·6H<sub>2</sub>O (Merck, Germany, 99%), HNO<sub>3</sub> (63%), NaOH (96%), ethanol (China), KNaC<sub>4</sub>H<sub>4</sub>O<sub>6</sub>·4H<sub>2</sub>O (50%), NH<sub>4</sub>Cl (Merck), Nessler reagent (Merck), argon gas, deionized water, and coffee husk.

Experimental equipment includes a UV-VIS 730 spectrophotometer (Japan), an IKA horizontal shaker, a CDC401-HACH handheld pH meter, an Ohaus drying oven (USA), a centrifuge, an oven and an analytical balance.

### 2.2. Composite materials manufacturing

To prepare activated carbon (AC), coffee husks were repeatedly washed with distilled water to remove impurities. The cleaned coffee husks were then dried in an oven at 110 °C for 24 hours and crushed to a uniform particle size of 0.5–1 mm. The coffee husks were subsequently soaked in a HNO<sub>3</sub> solution at 80 °C for 4 hours. The HNO<sub>3</sub> concentration used was 3 M, with an impregnation ratio (weight/volume) of coffee husk to HNO<sub>3</sub> at 1:10 [12]. The solid material was washed multiple times with distilled water until the pH stabilized at 7–8 and then dried at 70 °C to a constant weight. Next, 10

g of the blended coffee husks were placed in a porcelain cup and heated at 350 °C for 60 minutes in a furnace under an argon gas, with a controlled heating rate of 5 °C/min.

To synthesize MnFe<sub>2</sub>O<sub>4</sub> (MFO), a salt solution of MnCl<sub>2</sub>·4H<sub>2</sub>O (50 mL) and a salt solution FeCl<sub>3</sub>·6H<sub>2</sub>O (50 mL) was prepared in distilled water with an Mn<sup>2+</sup> to Fe<sup>3+</sup> molar ratio of 0.1:0.2 M in a conical flask (Flask 1). The mixture was stirred for 90 min using a magnetic stirrer. Simultaneously, 65 mL of NaOH solution (2 M) was prepared in another conical flask (Flask 2). Both flasks were then heated in a water bath until the temperature of the solutions reached 80 °C. The solution from Flask 1 was carefully poured into Flask 2 while maintaining constant agitation, and the mixture was stirred at 80 °C for an additional 90 minutes [10]. We see a black precipitate appearing, which is the MnO·Fe<sub>2</sub>O<sub>3</sub> (MnFe<sub>2</sub>O<sub>4</sub>) precipitate. The resulting mixture was filtered, and the precipitate was thoroughly washed with distilled water until a neutral pH (pH = 7) was achieved. The final precipitate was dried at 80 °C for 24 hours and labeled as MFO.

To synthesize the MFO/AC nanocomposite, MnFe<sub>2</sub>O<sub>4</sub> and coffee husk-derived activated carbon were mixed in various ratios of 1:3% by weight. The mixtures were prepared in conical flasks using both co-precipitation and hydrothermal methods simultaneously. Subsequently, 70 mL of double-distilled water was added to each flask, and the contents were stirred for three hours using a magnetic stirrer. The flasks were then transferred to a Teflon-lined stainless-steel autoclave and subjected to hydrothermal treatment at 200 °C for 12 h. After the hydrothermal process, the samples were allowed to cool to room temperature, centrifuged until reaching a neutral pH (pH = 7), and then dried at 80 °C to a constant weight.

### 2.3. Adsorption experiments

The ammonium adsorption capacity of the MFO/AC nanocomposite was assessed under various conditions, including pH (3÷8), contact time (5÷120 minutes), adsorbent dosage (0.2–3 g/L), and ammonium solution concentrations (10÷60 mg.L<sup>-1</sup>). The initial ammonium concentration for the experiments was set at 20 mg.L<sup>-1</sup>. Adsorption experiments were conducted in a beaker with continuous stirring at 120 rpm using a horizontal shaker under room temperature conditions (25 ± 2 °C). After the adsorption process, the samples were allowed to settle, and filtered, and the ammonium concentration was determined at a wavelength of 450 nm using the standard calibration curve  $y = 0.1053x - 0.0004$  with  $R^2 = 0.9991$ . Each experiment was repeated three times, and the average values were calculated for analysis and evaluation.

The adsorption capacity was calculated using equation (1), while the adsorption efficiency was determined using equation (2):

$$q_e = \frac{(C_o - C_e)V}{m} \quad (1)$$

$$H = \frac{(C_o - C_e)}{C_o} \times 100\% \quad (2)$$

where:  $q_e$ : adsorption capacity of the material (mg.g<sup>-1</sup>);  $C_o$ : initial ammonium concentration (mg.L<sup>-1</sup>);  $C_e$ : residual ammonium concentration in the test solution (mg.L<sup>-1</sup>);  $V$ : volume of solution (L);  $m$ : mass of material (g).

Data analysis was conducted using Excel software, while graphs and adsorption modeling were performed with Origin 2019 software. The data presented in the graphs are expressed as the mean ± standard deviation.

### 3. Results and discussion

#### 3.1. The surface structure of the material

The SEM image in Figure 1 shows that activated carbon (AC) morphology was inert, had large particle size, and had few pores (Figure 1a). In contrast, the surface of MFO/AC displayed small reflective particles unevenly dispersed on a smooth and porous substrate (Figure 1b). This indicates that the composite process facilitated the adhesion of  $MnFe_2O_4$  particles to the surface of activated carbon, resulting in a composite material with enhanced porosity and a smoother surface.

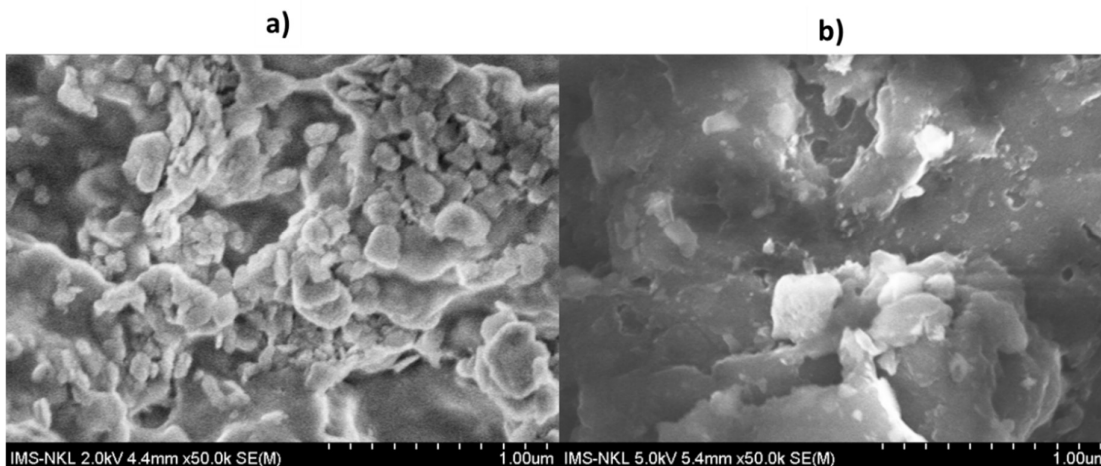


Figure 1. The SEM images of AC (a) and MFO/AC (b).

The results in Figure 2 show the presence of  $-OH$  group stretching vibration at  $3439\text{ cm}^{-1}$  in  $MnFe_2O_4$  and  $3424\text{ cm}^{-1}$  in MFO/AC. On the  $MnFe_2O_4$  surface, the peak at  $432\text{ cm}^{-1}$  and  $634\text{ cm}^{-1}$  corresponds to the vibration of the Fe-Mn-O bond in the material [13]. On the MFO/AC surface, a broad ridge at  $2926\text{ cm}^{-1}$  is attributed to C-H stretching vibration under alkaline conditions. Additionally, the presence of a C-O group was observed at  $1384\text{ cm}^{-1}$ , while the peak at  $1618\text{ cm}^{-1}$  is associated with C=C groups [14] in MFO/AC. Notably, the adsorption peak at  $634\text{ cm}^{-1}$  for  $MnFe_2O_4$  shifted slightly to  $574\text{ cm}^{-1}$  in MFO/AC, indicating the vibration of the Fe-Mn-O bond [13].

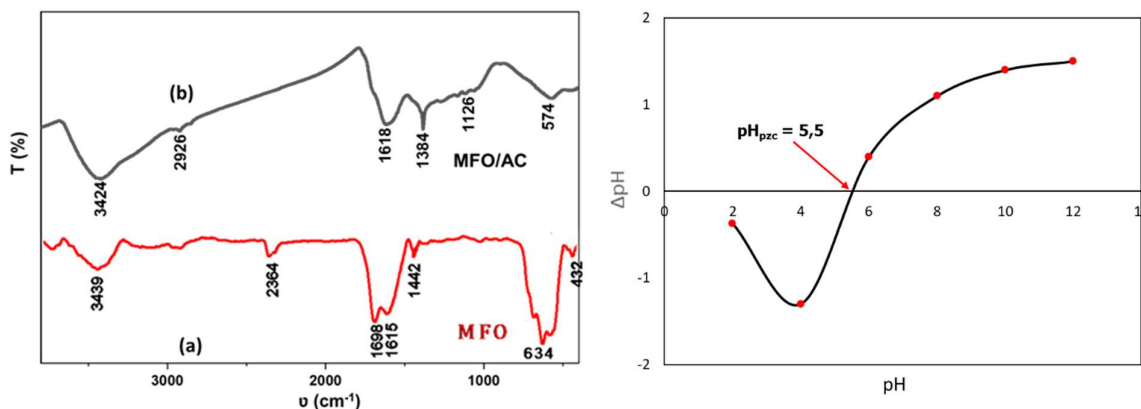


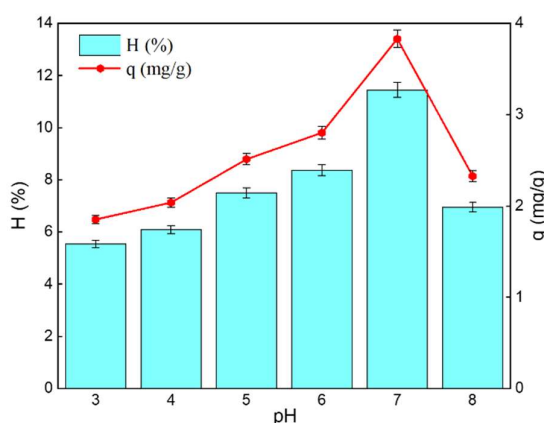
Figure 2. FTIR spectrum of  $MnFe_2O_4$  (a) and  $MnFe_2O_4/AC$  (b).

Figure 3.  $\text{pH}_{\text{PZC}}$  of  $MnFe_2O_4/AC$ .

The isoelectric point ( $\text{pH}_{\text{PZC}}$ ) is a critical parameter in understanding the adsorption of ions from a solution onto the surface of solids. The  $\text{pH}_{\text{PZC}}$  of the MFO/AC composite material, as determined from the results shown in Figure 3, was found to be 5.5, indicating a weakly acidic surface. When the pH of the solution is less than  $\text{pH}_{\text{PZC}}$ , the surface of the composite material becomes positively charged, enhancing the adsorption of anions. Conversely, when the pH exceeds  $\text{pH}_{\text{PZC}}$ , the surface becomes negatively charged, favoring the adsorption of cations [15]. This  $\text{pH}_{\text{PZC}}$  value provides a fundamental basis for understanding and explaining the adsorption mechanism of ammonium ions in water by the MFO/AC composite material.

### 3.2. Factors influencing the ammonium adsorption capacity of MFO/AC

#### 3.2.1. Effect of pH on ammonium adsorption capacity



**Figure 4.** Effect of pH on ammonium adsorption capacity of MFO/AC (at contact time 20 minutes, adsorbent dosage  $0.6 \text{ g} \cdot \text{L}^{-1}$  and  $C_0 = 20 \text{ mg} \cdot \text{L}^{-1}$ ).

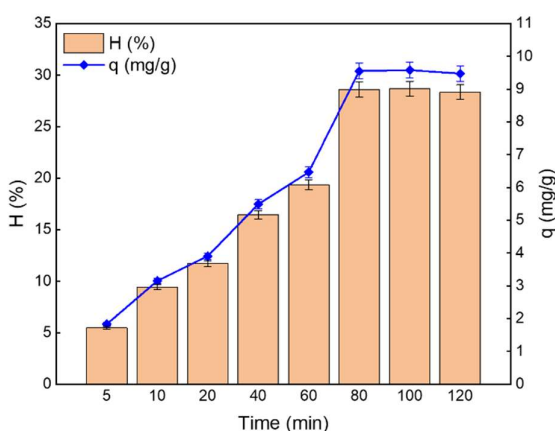


**Figure 5.** Effect of time on ammonium adsorption capacity (at  $\text{pH} = 7$ , adsorbent dosage  $0.6 \text{ g} \cdot \text{L}^{-1}$  and  $C_0 = 20 \text{ mg} \cdot \text{L}^{-1}$ ).

The results in Figure 4 indicate that as the pH value of the solution increases from 3 to 7, the ammonium adsorption capacity of MFO/AC gradually increases, reaching its highest value at pH 7, with an adsorption capacity ( $q$ ) of  $3.83 \text{ mg} \cdot \text{g}^{-1}$  and an ammonium removal efficiency of 11.48%. However, as the pH increases further (from 7 to 8), the ammonium adsorption capacity of the material decreases sharply. This can be explained as follows: at a pH range of 6–7, ammonium predominantly exists in the form of  $\text{NH}_4^+$  [16], while the MFO/AC material surface is negatively charged due to its  $\text{pH}_{\text{PZC}}$  value of 5.5 (Figure 3). Consequently, the negatively charged MFO/AC surface electrostatically attracts  $\text{NH}_4^+$ , leading to a rapid increase in ammonium adsorption capacity, peaking at pH 7. When the pH exceeds 7, the ammonium adsorption capacity decreases sharply due to the increasing concentration of  $\text{OH}^-$  ions in the solution. In addition, when  $\text{pH} > 7$ , part of  $\text{NH}_4^+$  is converted to  $\text{NH}_3$ , which is less effectively adsorbed. These findings confirm that the primary mechanism of ammonium adsorption on MFO/AC is surface adsorption through electrostatic attraction between the negatively charged MFO/AC surface and  $\text{NH}_4^+$  ions in the solution. This result aligns with the findings of A. Alshameri et al. [17] and X.G. Wang et al. [18]. Based on these findings, the optimal pH for this study was determined to be 7.

#### 3.2.2. Effect of time on ammonium adsorption capacity

The results in Figure 5 demonstrate that adsorption time significantly influenced the ammonium adsorption capacity on the MFO/AC surface. During the initial 5–80 min, the ammonium adsorption

capacity of the material increased rapidly, from  $1.83 \text{ mg}\cdot\text{g}^{-1}$  to  $9.55 \text{ mg}\cdot\text{g}^{-1}$ , corresponding to an increase in treatment efficiency from 5.5 % to 28.6 %. The adsorption capacity then gradually stabilized during the 80–120 minute period with the adsorption capacity fluctuating slightly from 9.47 to  $9.58 \text{ mg}\cdot\text{g}^{-1}$ , corresponding to an adsorption efficiency ranging from 28.4 to 28.7%. At  $t = 80 \text{ min}$ , the ammonium adsorption capacity of MFO/AC reached  $9.55 \text{ mg}\cdot\text{g}^{-1}$ , with a treatment efficiency of 28.6 %. Based on these findings, the optimal adsorption time for this study was determined to be 80 min.

### 3.2.3. The effect of the MFO/AC content on the adsorption efficiency of ammonium

The increase in ammonium adsorption efficiency of the adsorbents was attributed to the rise in the number of available adsorption sites. However, beyond a certain point, the adsorption efficiency reached its maximum and further increases in adsorbent content did not significantly improve. The results in Figure 6 indicate that within the adsorbent dosage range of  $0.2\text{--}1.5 \text{ g}\cdot\text{L}^{-1}$ , the adsorption efficiency for ammonium increased from 11.9% to 43.8% and then gradually stabilized in the range of  $1.5\text{--}3 \text{ g}\cdot\text{L}^{-1}$  with adsorption efficiency fluctuating slightly from 43.4 to 43.8%. Based on the ammonium adsorption efficiency (H%), the MFO/AC content of  $1.5 \text{ g}\cdot\text{L}^{-1}$  was selected for subsequent experiments.

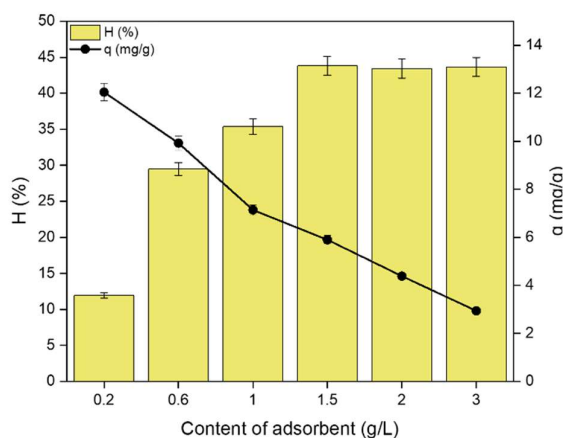


**Figure 6.** Effect of adsorbent content on ammonium adsorption capacity (at  $\text{pH} = 7$ , contact time 80 minutes and  $C_0 = 20 \text{ mg}\cdot\text{L}^{-1}$ ).

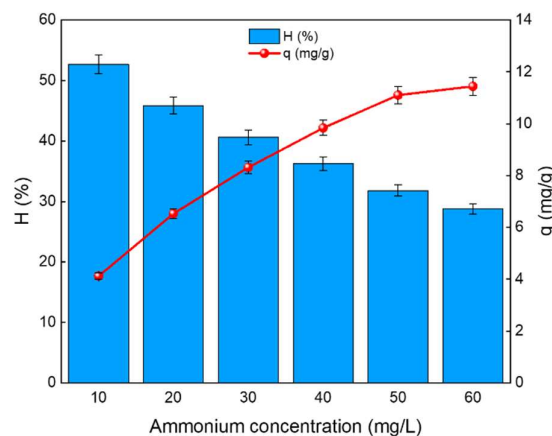


**Figure 7.** Effect of ammonium concentrations on ammonium adsorption capacity (at  $\text{pH} = 7$ , contact time 80 minutes, and adsorbent dosage  $1.5 \text{ g}\cdot\text{L}^{-1}$ ).

### 3.2.4. Effect of initial concentration of ammonium on adsorption efficiency

The results in Figure 7 indicate that as the initial ammonium concentration increases, the ammonium treatment efficiency decreases, whereas the ammonium adsorption capacity increases. These findings are consistent with the theoretical predictions based on equations (1) and (2).

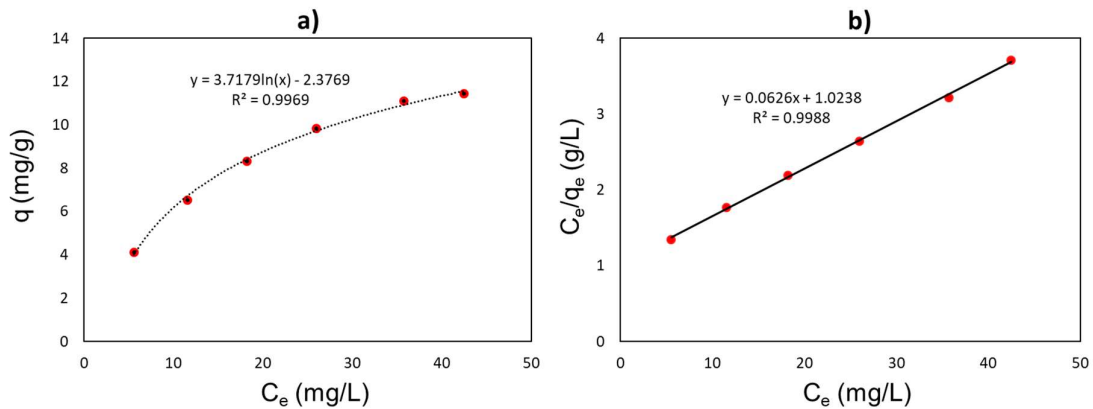


**Figure 8.** Langmuir Isothermal adsorption of adsorbent for ammonium (a) and  $C_e/q$  dependence on  $C_e$  for ammonium (b).

Isothermal adsorption is a mathematical model used to describe the distribution of ammonium in water, based on the assumption of homogeneous or nonhomogeneous characteristics of the adsorbent. Since the adsorption process occurs in an aqueous medium, the Langmuir model is the most commonly applied due to its higher accuracy [19]. Experimental results showed that the ammonium adsorption by the material conforms to the Langmuir isothermal adsorption model:  $\frac{C_e}{q} = \frac{1}{q_m} C_e + \frac{1}{q_m \cdot b}$  (3) as shown in Figure 8b.

Where:  $C_e$ : residual metal concentration in the test solution ( $\text{mg}\cdot\text{L}^{-1}$ );  $q$ : adsorption capacity of the material ( $\text{mg}\cdot\text{g}^{-1}$ );  $q_m$ : maximum adsorption capacity of the material ( $\text{mg}\cdot\text{g}^{-1}$ );  $b$ : Langmuir constant.

From Figure 8b, the maximum adsorption capacity of ammonium can be calculated using the slope of the linear plot:  $q_m = \frac{1}{\tan \alpha} = \frac{1}{0.0626} = 15.97$  ( $\text{mg}\cdot\text{g}^{-1}$ ). The results showed that the maximum ammonium adsorption capacity of MFO/AC was  $15.97 \text{ mg}\cdot\text{g}^{-1}$ , with a Langmuir constant of 0.06.

Compared with similar composite materials, the MFO/AC sample demonstrated a higher ammonium adsorption capacity than other adsorbents, such as the NaOH-modified ball-milled biochar (maximum adsorption capacity:  $8.93 \text{ mg}\cdot\text{g}^{-1}$ ) [20], Montmorillonite/ $\text{Fe}_3\text{O}_4$  nanocomposite (maximum adsorption capacity:  $10.48 \text{ mg}\cdot\text{g}^{-1}$ ) [21], and biochar derived from post-extraction coffee bean grounds (maximum adsorption capacity:  $14.48 \text{ mg}\cdot\text{g}^{-1}$ ) [22].

#### 4. Conclusion

This study successfully synthesized the composite materials combining  $\text{MnFe}_2\text{O}_4$  and activated carbon from coffee husks (MFO/AC) using co-precipitation and hydrothermal methods. The MFO/AC composite material was investigated for its ammonium adsorption capability in water, considering factors such as pH, adsorption time, adsorbent dosage and initial ammonium concentration. Under optimal conditions (pH = 7, adsorption time = 80 min and adsorbent dosage =  $1.5 \text{ g}\cdot\text{L}^{-1}$ ), the maximum ammonium adsorption capacity of the material was determined to be  $15.97 \text{ mg}\cdot\text{g}^{-1}$ . Compared with similar composite materials, the MFO/AC sample demonstrated a higher ammonium adsorption capacity than other adsorbents.

## Acknowledgments

This research is funded by Hanoi Pedagogical University 2 Foundation for Sciences and Technology Development under Grant number HPU2.2023-UT.15.

## References

- [1] E. Stokstad, "Air pollution ammonia pollution from farming may exact hefty health costs," *Science*, vol. 343, no. 6168, Jan. 2014, Art. no. 238, doi: 10.1126/science.343.6168.238.
- [2] A.T. Puari, N. Rusnam, and N.R. Yanti, "Removal of Ammonium by Biochar Derived from Exhausted Coffee Husk (ECH) at Different Carbonisation Parameter," *IOP Conf. Ser. Earth Environ. Sci.*, vol. 1182, no. 1, Jun. 2023, Art. no. 012037, doi: 10.1088/1755-1315/1182/1/012037.
- [3] E. Blázquez, T. Bezerra, J. Lafuente, and D. Gabriel, "Performance, limitations and microbial diversity of a biotrickling filter for the treatment of high loads of ammonia," *Chem. Eng. J.*, vol. 311, pp. 91–99, Mar. 2017, doi: 10.1016/j.cej.2016.11.072.
- [4] M. R. Adam *et al.*, "Current trends and future prospects of ammonia removal in wastewater: A comprehensive review on adsorptive membrane development," *Sep. Purif. Technol.*, vol. 213, pp. 114–132, Apr. 2019, doi: 10.1016/j.seppur.2018.12.030.
- [5] F. Liao, G. Diao, and H. Li, "Green synthesis of graphene oxide-MnFe<sub>2</sub>O<sub>4</sub> composites and their application in removing heavy metal ions," *Micro Nano Lett.*, vol. 15, no. 1, pp. 7–12, Jan. 2020, doi: 10.1049/mnl.2018.5640.
- [6] K. Asghar, M. Qasim, and D. Das, "Preparation and characterization of mesoporous magnetic MnFe<sub>2</sub>O<sub>4</sub>@mSiO<sub>2</sub> nanocomposite for drug delivery application," *Mater. Today Proc.*, vol. 26, no.1, pp. 87-93, Jul. 2019, doi: 10.1016/j.matpr.2019.05.380.
- [7] M.S. Podder and C. B. Majumder, "Application of granular activated carbon/MnFe<sub>2</sub>O<sub>4</sub> composite immobilized on C. glutamicum MTCC 2745 to remove As(III) and As(V): Kinetic, mechanistic and thermodynamic studies," *Spectrochim. Acta - Part A Mol. Biomol. Spectrosc.*, vol. 153, pp. 298–314, Aug. 2015, doi: 10.1016/j.saa.2015.08.022.
- [8] M. A. M. Taguba *et al.*, "Nonlinear Isotherm and Kinetic Modeling of Cu(II) and Pb(II) Uptake from Water by MnFe<sub>2</sub>O<sub>4</sub>/Chitosan Nanoadsorbents," *Water*, vol. 13, no. 12, Jun. 2021, Art. no. 1662, doi: 10.3390/w13121662.
- [9] P. T. L. Huong *et al.*, "Functional manganese ferrite/graphene oxide nanocomposites: effects of graphene oxide on the adsorption mechanisms of organic MB dye and inorganic As(v) ions from aqueous solution," *RSC Adv*, vol. 8, no. 22, pp. 12376–12389, 2018, doi: 10.1039/c8ra00270c.
- [10] T. V. Tuyen *et al.*, "Carbon-encapsulated MnFe<sub>2</sub>O<sub>4</sub> nanoparticles: effects of carbon on structure, magnetic properties and Cr(VI) removal efficiency," *Appl Phys Mater Sci Process*, vol. 126, no. 7, pp. 577–589, Jul. 2020, doi: 10.1007/s00339-020-03760-7.
- [11] J. Wan, H. Deng, J. Shi, L. Zhou, and T. Su, "Synthesized Magnetic Manganese Ferrite Nanoparticles on Activated Carbon for Sulfamethoxazole Removal," *Clean - Soil, Air, Water*, vol. 42, no. 9, pp. 1199–1207, Mar. 2014, doi: 10.1002/clen.201300432.
- [12] D. T. Tien, T. V. Tuyen, N. K. Chi, "Experimental results of adsorption of Ni (II) from wastewater using coffee husk-based activated carbon," *Vietnam Journal of Science and Technology*, vol. 56, no.2C, pp. 126–132, Aug. 2018, doi: 10.15625/2525-2518/56/2c/13039.
- [13] A. Mary Jacintha, V. Umapathy, P. Neeraja, and S. Rex Jeya Rajkumar, "Synthesis and comparative studies of MnFe<sub>2</sub>O<sub>4</sub> nanoparticles with different natural polymers by sol–gel method: structural, morphological, optical, magnetic, catalytic and biological activities," *J. Nanostructure Chem.*, vol. 7, no. 4, pp. 375–387, Nov. 2017. doi: 10.1007/s40097-017-0248-z.
- [14] Y. Yang *et al.*, "ZnO nanoparticles loaded rice husk biochar as an effective adsorbent for removing reactive red 24 from aqueous solution," *Mater Sci Semicond Process*, vol. 150, Nov. 2022, Art. no. 106960, doi: 10.1016/j.mssp.2022.106960.
- [15] M. Kosmulski, "The pH dependent surface charging and points of zero charge," *VII. Update. Adv. Colloid Interface Sci.*, vol. 251, pp. 115–138, Jan. 2018, doi: 10.1016/j.cis.2017.10.005.
- [16] E. Marañón, M. Ulmanu, Y. Fernández, I. Anger, and L. Castrillón, "Removal of ammonium from aqueous solutions with volcanic tuff," *Journal of Hazardous Materials*, vol. 137, no. 3, pp. 1402–1409, Oct. 2006, doi: 10.1016/j.jhazmat.2006.03.069.

- [17] A. Alshameri *et al.*, “Adsorption of ammonium by different natural clay minerals: Characterization, kinetics and adsorption isotherms,” *Applied Clay Science*, vol. 159, pp. 83–93, Jun. 2018, doi: 10.1016/j.clay.2017.11.007.
- [18] X. G. Wang *et al.*, “Recovery of ammonium and phosphate from wastewater by wheat straw-based amphoteric adsorbent and reusing as a multifunctional slow-release compound fertilizer,” *ACS Sustain. Chem. Eng.*, vol. 4, no. 4, pp. 2068–2079, Mar. 2016, doi: 10.1021/acssuschemeng.5b01494.
- [19] L. H. Nguyen, T. M. Vu, T. T. Le, V. T. Trinh, T. P. Tran, and H. T. Van, “Ammonium removal from aqueous solutions by fixed-bed column using corncob-based modified biochar,” *Environmental Technology*, vol. 40, no. 6, pp. 683–692, Nov. 2019, doi: 10.1080/09593330.2017.1404134.
- [20] H. Yang *et al.*, “Effective Removal of Ammonium from Aqueous Solution by Ball-Milled Biochar Modified with NaOH,” *Processes*, vol. 11, no. 6, May 2023, Art. no. 1671, doi: 10.3390/pr11061671.
- [21] J. Song, V. Srivastava, T. Kohout, M. Sillanpää, and T. Sainio, “Montmorillonite-anchored magnetite nanocomposite for recovery of ammonium from stormwater and its reuse in adsorption of  $\text{Sc}_3^+$ ,” *Nanotechnol. Environ. Eng.*, vol. 6, no. 3, pp. 1–14, Sep. 2021, doi: 10.1007/s41204-021-00151-y.
- [22] H. L. Nguyen *et al.*, “Biochar of post-extraction coffee bean ground as materials for ammonium adsorption,” *Vietnam Journal of Science and Technology*, vol. 62, no. 2, pp. 324–334, Mar. 2024, doi: 10.15625/2525-2518/17989.